Predisposition to late-onset obesity in GIRK4 knockout mice

Cydne A. Perry*, Marco Pravetoni*, Jennifer A. Teske†, Carolina Aguado‡, Darin J. Erickson§, Juan F. Medrano¶, Rafael Luján‡, Catherine M. Kotz†, and Kevin Wickman*‖

*Department of Pharmacology, University of Minnesota, 6-120 Jackson Hall, 321 Church Street SE, Minneapolis, MN 55455; †Minnesota Obesity Center, Department of Food Science and Nutrition, Veterans Affairs Medical Center, Geriatric Research Education and Clinical Center, 11G, One Veterans Drive, Minneapolis, MN 55417; ‡Departmento de Ciencias Médicas, Campus Biosanitario C/Almansa, Universidad de Castilla–La Mancha, 14, 02006 Albacete, Spain; §Division of Epidemiology, School of Public Health, University of Minnesota, 1300 South Second Street, Suite 300, Minneapolis, MN 55454; and ¶Department of Animal Science, University of California, 1 Shields Avenue, Davis, CA 95616

G protein-gated inwardly rectifying potassium (GIRK/Kir3) channels mediate the inhibitory effects of many neurotransmitters on excitable cells. Four *Girk* genes have been identified (*Girk1–4*). Whereas GIRK4 is associated with the cardiac GIRK channel, *Girk4* expression has been detected in a few neuron populations. Here, we used a transgenic mouse expressing enhanced green fluorescent protein (EGFP) under the control of the *Girk4* gene promoter to clarify the expression pattern of *Girk4* in the brain. Although small subsets of EGFP-positive neurons were evident in some areas, prominent labeling was seen in the hypothalamus. EGFP expression was most pronounced in the ventromedial, paraventricular, and arcuate nuclei, neuron populations implicated in energy homeostasis. Consistent with a contribution of GIRK4-containing channels to energy balance, *Girk4* knockout (−/−) mice were predisposed to late-onset obesity. By 9 months, *Girk4⁻/⁻* mice were ≈25% heavier than wild-type controls, a difference attributed to greater body fat. Before the development of overweight, *Girk4⁻/⁻* mice exhibited a tendency toward greater food intake and an increased propensity to work for food in an operant task. *Girk4⁻/⁻* mice also exhibited reduced net energy expenditure, despite displaying elevated resting heart rates and core body temperatures. These data implicate GIRK4-containing channels in signaling crucial to energy homeostasis and body weight.

body weight | energy balance | hypothalamus | Kir3

G protein-gated inwardly rectifying K⁺ (GIRK/Kir3) channels mediate the slow inhibitory effect of neurotransmitters and hormones on excitable cells of the heart and nervous system (1). GIRK channels are gated by the Gβγ subunits of the Gi/o subclass of heterotrimeric G proteins (2) and are homo- and heterotetrameric complexes formed by four related subunits (GIRK1–4) (3, 4). Neuronal GIRK channels are thought to consist of various combinations of GIRK1, GIRK2, and GIRK3 channel subunits (5). In contrast, the cardiac GIRK channel (I$_{KACh}$) is a heterotetramer consisting of GIRK1 and GIRK4 (4).

Girk4⁻/⁻ mice exhibit a complete loss of cardiac GIRK channel activity and cardiac deficits including a mild resting tachycardia and blunted reflex bradycardia (6), consistent with the known expression pattern of the *Girk4* gene (also known as *Kcnj5*) (7). By careful comparison of tissue from wild-type and *Girk4⁻/⁻* mice, a small number of neuron populations in the adult mouse were identified that express *Girk4* (8). Signal intensity was particularly high in the ventromedial hypothalamus, a region that contains the ventromedial (VMN) and arcuate (ARC) nuclei.

The hypothalamus is central to the regulation of food intake and energy expenditure. Early studies suggested that the ventromedial and lateral hypothalamus functioned as satiety and feeding centers, respectively (9). More recent work has shown that orexin neurons in the lateral hypothalamus and neuropeptide Y (NPY)-positive neurons of the ARC are critical for the initiation of feeding (10). Conversely, the VMN and pro-opiomelanocortin (POMC) neurons in the ARC are key neuronal substrates of satiety and enhanced

energy expenditure. Although GIRK channels have been implicated in the postsynaptic inhibition of hypothalamic neurons, the subunit composition(s) of the underlying GIRK channel has not been elucidated (e.g. refs. 11 and 12).

Given its otherwise limited tissue distribution, the expression of the *Girk4* gene in the ventromedial hypothalamus suggested that GIRK4-containing channels might make important contributions to energy homeostasis. Accordingly, we sought to clarify the expression pattern of *Girk4* in the hypothalamus and to examine the impact of *Girk4* ablation on body weight, food intake, and energy expenditure. Our findings indicate that GIRK4-containing ion channels make a significant contribution to signaling pathways charged with maintaining energy homeostasis.

Results

We demonstrated by *in situ* hybridization that the *Girk4* gene is expressed in only a few neuron populations, with conspicuous labeling seen in the ventromedial hypothalamus (8). To validate observation, we acquired a transgenic mouse line [Tg(*Kcnj5*-EGFP)49Gsat] that expresses EGFP under the control of the *Girk4* promoter. Cardiac tissue from transgene-positive animals exhibited robust EGFP expression (Fig. 1 *A* and *B*). EGFP was expressed in both atrial and ventricular tissue, with fluorescence notably more intense in the atria. Thus, EGFP expression in Tg(*Kcnj5*-EGFP)49Gsat mice provides an accurate readout of *Girk4* gene expression in the heart (8).

EGFP labeling in brain sections from Tg(*Kcnj5*-EGFP)49Gsat mice confirmed the limited expression of the *Girk4* gene in the CNS. EGFP expression was found in small subsets of cells in defined structures, including the substantia nigra and hippocampus (Fig. 1 *C* and *D*), and cerebellum (13). In contrast, EGFP labeling in the hypothalamus was prominent and relatively uniform. EGFP intensity was highest in the VMN, although robust expression was also seen in the paraventricular nucleus (PVN) and posterior aspect of the ARC (Table 1 and Fig. 2). Quantification of the overlap between EGFP and the neuron-specific nuclear marker NeuN revealed that most neurons in the VMN (85%), posterior ARC (78%), and PVN (74%) were EGFP-positive [supporting information (SI) Fig. S1].

Given the relevance of the VMN, ARC, and PVN to energy homeostasis, we sought to determine whether genetic ablation of *Girk4* influenced body weight (Fig. 3). The *Girk4⁻/⁻* mouse line was created by using embryonic stem cells derived from the 129S1/
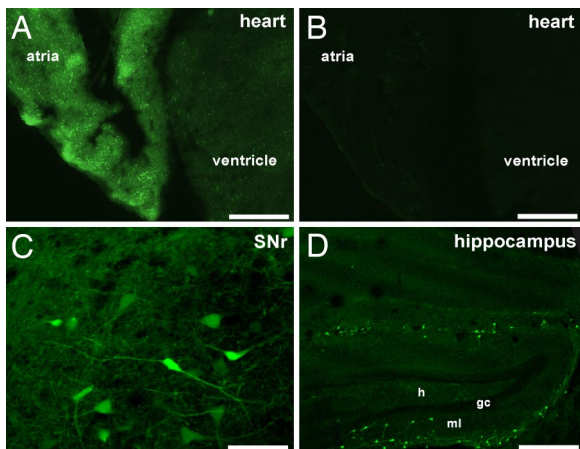
Fig. 1. EGFP expression in the Tg(*Kcnj5*-EGFP)49Gsat mouse. (*A* and *B*) EGFP signal was observed in sections (15 μm) from transgene-positive (Tg+) (*A*) but not transgene-negative (Tg−) (*B*) mice. (Scale bars: 1 mm.) (*C* and *D*) Sections containing the substantia nigra pars reticulata (*C*) (SNr) and hippocampus (*D*). The neurons found in the dentate gyrus may be MOPP cells described by Somogyi and colleagues (33). h, hilus; ml, molecular layer; gc, granule cell layer. (Scale bars: *C*, 50μm; *D*, 300μm.)

Table 1. EGFP expression in the hypothalamus

Nucleus	Abbreviation	Expression
Ventromedial hypothalamic nucleus	VMN	+++++
Paraventricular hypothalamic nucleus		
anterior parvicellular	PaAP	++++
ventral	PaV	+
lateral magnocellular	PaLM	++++
medial magnocellular	PaMM	+++
dorsal (cap)	PaD	+++
posterior	PaPo	++++
sub-paraventricular zone	SPa	+++
Arcuate nucleus, lateral	ArcL	++
Arcuate nucleus, dorsal	ArcD	+
Arcuate nucleus, posterior	ArcP	++++
Anterodorsal preoptic nucleus	ADP	+++
Lateroanterior hypothalamic nucleus	LA	+++
Supramammillary nucleus	SuMM	+++
Supramammillary nucleus, lateral	SUML	+++
Dorsal tuberomammillary nucleus	DTM	++
Medial preoptic area	MPA	++
Perifornical nucleus	PeF	++
Periventricular hypothalamic nucleus	Pe	++
Reuniens thalamic nucleus	Re	++
Suprachiasmatic nucleus	SCh	++
Zona incerta	ZI	++
Dorsomedial hypothalamic nucleus	DM	+
Lateral hypothalamic area	LH	+
Lateral mammillary nucleus	LM	+
Medial tuberal nucleus	MTu	+
Premammillary nucleus, ventral	PMV	+
Posterior hypothalamic area	PH	+
Anterior hypothalamic area, central	AHC	+
Anterior hypothalamic area, posterior	AHP	+

EGFP expression levels were determined by fluorescence microscopy in coronal sections. Nuclei were identified based upon morphological criteria and published coordinates for the adult mouse. Labeling intensities: +++++, highest; ++++, very strong; +++, strong; ++, moderate; +, weak. Results are based on findings from three transgenic mice. EGFP was not detected in the median eminence (ME), anterior hypothalamic area (anterior, AHA), medial mammillary nucleus (lateral, ML; median, MMn; or medial, MM), mammillothalamic tract (mt), lateral preoptic area (LPO), or fornix (f).

SvImJ inbred strain (14). Before evaluating body weight, the *Girk4* null mutation was backcrossed for 22 generations against the C57BL/6J inbred strain. Fine mapping revealed that the *Girk4* null allele was flanked by between 3.8 Mbp (30.2–34.0 Mbp) and 5.3 Mbp (29.7–35.0 Mbp) of residual 129/SvImJ sequence, also referred to as the differential chromosome segment (*SI Text* and Table S1). This region contains 13–19 genes (Table S2). Because 129/SvImJ mice exhibit lower body weights and body fat content than C57BL/6J mice (15), any contribution of the minimal residual 129/SvImJ-based genomic sequence to phenotypic expression would be predicted to favor a lean phenotype.

Body weights of group-housed *Girk4⁻/⁻* mice mirrored those of wild-type controls from 3 weeks to 2 months of age (Fig. 3*A*). Genotype-dependent differences developed between 3 and 9 months of age, however, such that *Girk4⁻/⁻* mice were ≈25–30% heavier than their wild-type counterparts (Fig. 3 *B* and *C*). Interestingly, the coefficient of variation (CV%) linked to body weight was typically 2–4 times larger for *Girk4⁻/⁻* mice as compared with wild-type controls for any given time point, attesting to the large intersubject variability seen in the *Girk4⁻/⁻* group. A general linear mixed model analysis revealed an influence of gender [male > female, $t(137) = 4.08$; $P < 0.001$] and genotype [*Girk4⁻/⁻* > wild type, $t(137) = 4.81$; $P < 0.001$] on weight gain between 3 and 12 months; the interaction between gender and genotype was not significant. Naso-anal body length measurements were similar for wild-type and *Girk4⁻/⁻* mice (data not shown), suggesting that enhanced linear growth does not explain the overweight phenotype. Chemical (Soxhlet) analysis of body composition revealed significantly higher fat content in *Girk4⁻/⁻* mice at 12 months of age (Fig. 3*D*).

To determine whether the intersubject variability in body weight among *Girk4⁻/⁻* mice was unique to group-housing conditions, we tracked weight in a cohort of mice weaned into single housing at 8 weeks of age. Although single housing does influence behavior in C57BL/6 mice (16), the impact on body weight and food intake is relatively small (17). At separation, there was an effect of gender [$t(145) = 7.81$; $P < 0.001$] but not genotype [$t(145) = 0.57$; $P = 0.57$] on body weight. During acclimation (8–12 weeks), weight gain was similar across groups (≈2 g). Consistent with the group-housing study, males gained more weight than females [$t(145) = 2.08$; $P = 0.04$] and *Girk4⁻/⁻* mice gained more weight than controls [$t(145) = 3.05$; $P < 0.01$] between 12 and 36 weeks (Fig. 4 *A* and *B*).

Furthermore, the intersubject variability in body weights for male (CV% = 10–19) and female (CV% = 11–24) *Girk4⁻/⁻* mice was larger than that seen for male (CV% = 4–7) and female (CV% = 5–9) wild-type mice. Thus, elevated weight gain and intersubject variability in body weights for *Girk4⁻/⁻* mice are not linked to group housing. Nevertheless, only female *Girk4⁻/⁻* mice were heavier than wild-type counterparts at the end of the study (Fig. 4 *A* and *B*). This discrepancy may reflect a tendency toward lower baseline body weights for the cohort of male *Girk4⁻/⁻* mice evaluated in the single-housing study (Fig. 4*A*) or a unique sensitivity of male *Girk4⁻/⁻* mice to single-housing conditions.

Daily food intake for single-housed wild-type mice was slightly higher during acclimation than seen for the same animals between 13 and 36 weeks (Fig. 4 *C* and *D*). *Girk4⁻/⁻* mice, in contrast, showed stable intake values between 8 and 36 weeks. While average daily food intake for single-housed *Girk4⁻/⁻* mice tended to be higher than that of wild-type controls, differences were not observed consistently. A significant effect of genotype on cumulative food intake (12–36 weeks) was observed [*Girk4⁻/⁻* > wild type, $t(170) = 2.33$; $P < 0.05$], however, as was an interaction between gender and genotype [$t(170) = 2.46$; $P < 0.05$]. Indeed, genotype-dependent differences in cumulative food intake appeared larger for female than male subjects. Interestingly, when cumulative food intake was included in the original general linear mixed model as a covariate, we found that although intake was predictive of baseline body weight ($P < 0.001$) and weight gain ($P < 0.001$), the effect of gender and genotype on these parameters remained significant (*P*
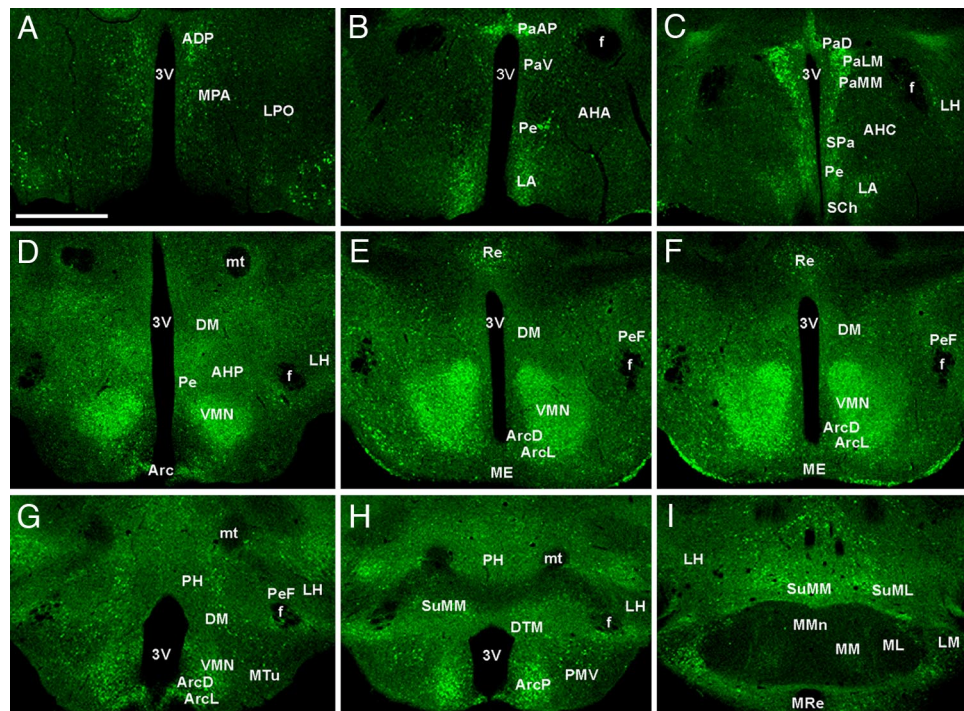
Fig. 2. EGFP expression in the hypothalamus of Tg(*Kcnj5*-EGFP)49Gsat mice. A series (rostral-to-caudal) of coronal sections (15 μm) through the hypothalamus from an adult male Tg(*Kcnj5*-EGFP)49sat mouse. Images are representative of those taken from three different Tg(*Kcnj5*-EGFP)49sat mice. Abbreviations are defined in Table 2. (Scale bar: 600 μm.)

value <0.05). Thus, enhanced intake alone is unable to account for the enhanced weight gain seen in *Girk4*$^{-/-}$ mice during this study.

We also measured the reinforcing effect of food in male wild-type and *Girk4*$^{-/-}$ mice using a three-phase operant task (18). Animals were subjected to mild food restriction to enhance operant responding; food restriction resulted in $\approx5\%$ reduction in free-feeding weight that did not differ between genotypes (data not shown). In phase 1, animals were trained to lever-press for food. The days required to satisfy acquisition criteria did not differ between
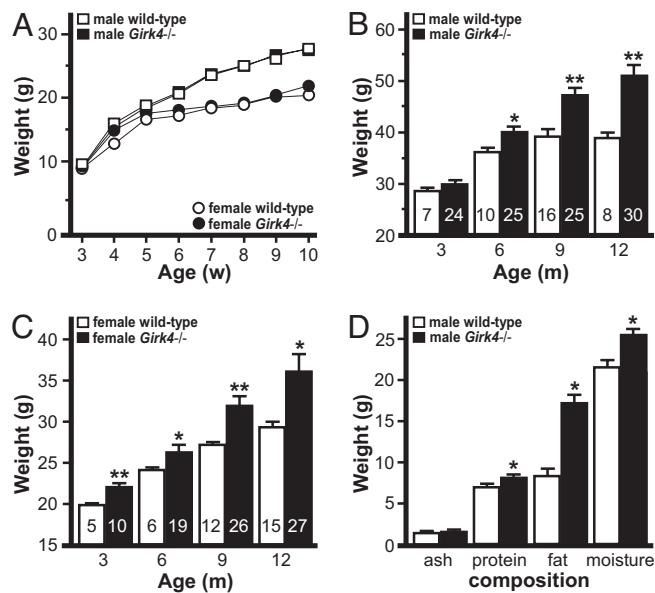

Fig. 3. Body weights of wild-type and *Girk4*$^{-/-}$ mice. (*A*) Body weights of wild-type and *Girk4*$^{-/-}$ mice at 3–10 weeks of age. Mice were housed with same-sex siblings (two to four per cage) of the same genotype. Groups ranged from 12 to 28 per genotype and gender. (*B* and *C*) Body weights of wild-type and *Girk4*$^{-/-}$ mice measured at 3, 6, 9, and 12 months of age. The number in each bar denotes the coefficient of variation (CV%). (*D*) Chemical (Soxhlet) analysis of carcass composition of 12-month-old male wild-type (*n* = 5) and *Girk4*$^{-/-}$ (*n* = 6) mice. ∗ and ∗∗, $P < 0.05$ and 0.01, respectively, vs. wild-type, same gender.
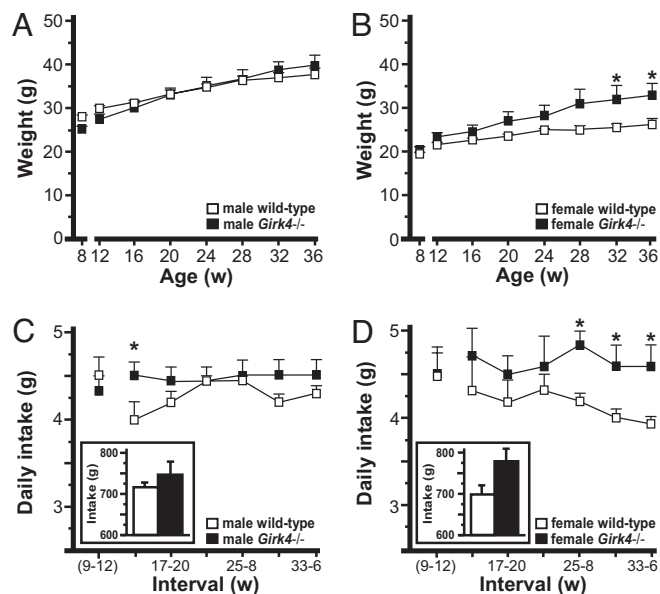

Fig. 4. Weight gain and food intake of single-housed wild-type and *Girk4*$^{-/-}$ mice. (*A* and *B*) Body weights of single-housed male (*A*) and female (*B*) wild-type and *Girk4*$^{-/-}$ mice between 12 and 36 weeks of age. (*C* and *D*) Daily food intake determined during 4-week intervals, including the acclimation period (weeks 9–12), for male (*C*) and female (*D*) wild-type and *Girk4*$^{-/-}$ mice. (*Insets*) Cumulative food intake between 13 and 36 weeks of age. Groups ranged from six to eight per genotype and gender. ∗, $P < 0.05$ vs. wild-type, same gender.

Table 2. Food-maintained operant responding

| | Phase 1 (FR1) | | | | Phase 2 (FR5) | | | Phase 3 (PR) | | | |
| | Lever presses | | | | Lever presses | | | Restricted | | Ad libitum | |
Group	Rate	Active	Inactive	Pellets	Active	Inactive	Pellets	Active	Pellets	Active	Pellets
Wild type	5.7 ± 0.5	92 ± 12	9 ± 3	63 ± 7	289 ± 38	13 ± 3	50 ± 5	738 ± 153	16.0 ± 1.0	216 ± 64	10.1 ± 1.2
Girk4−/−	5.9 ± 0.6	112 ± 11	8 ± 1	74 ± 6	325 ± 30	14 ± 3	58 ± 5	1,313 ± 128*	18.3 ± 0.7	366 ± 140	11.9 ± 0.9

The performance of male wild-type ($n = 7$) and Girk4−/− ($n = 13$) mice during acquisition (phase I, FR1), transition (phase 2, FR5), and progressive ratio (phase 3) components of the operant study. Mice were subjected to mild food restriction (3 g/day plus amount earned) during Phases 1, 2, and the food-restricted component of Phase 3. The rate to achieve acquisition (d), number of active and inactive lever presses, and pellets earned were averaged for each subject over the final 3 days of stable responding during Phases 1 and 2, and over the last 2 days of responding for Phase 3. Inactive lever responding did not differ during Phase 3 for wild-type and Girk4−/− mice (not shown). *, $P < 0.05$ vs. wild-type.

genotypes (Table 2). Girk4−/− mice did show slightly more active lever responding and pellets earned during phase 1 and phase 2, a transitional phase involving an FR 5 schedule of reinforcement. In phase 3, which involved progressive ratio scheduling (18), Girk4−/− mice displayed significantly elevated responding. Upon return to ad libitum feeding conditions, operant responding of Girk4−/− mice was greater, but not significantly different, than that seen for wild-type mice. Thus, caloric imbalance caused by food restriction influences operant responding in Girk4−/− mice.

Decreased energy expenditure could also contribute to the late-onset overweight phenotype seen in Girk4−/− mice. Given the role for GIRK4 in the formation of I$_{KACh}$, we evaluated heart rate and core body temperature by telemetry in wild-type and Girk4−/− mice at 3, 6, and 9 months of age. Core body temperature was consistently higher in Girk4−/− mice, and significant differences were observed at 3 and 6 months (Fig. 5A). Girk4−/− mice exhibited a resting tachycardia at all time points evaluated (Fig. 5B). Thus, with respect to these endpoints, Girk4−/− mice show evidence of an increase, rather than a decrease, in energy expenditure.

We next measured net energy expenditure in wild-type and Girk4−/− mice using indirect calorimetry. Animals were evaluated at 2–4 months to determine whether genotype-dependent differences in energy expenditure preceded the development of overweight. Spontaneous physical activity was measured together with O$_2$ consumption and CO$_2$ production during a 22.5-h session. No significant differences between genotypes were observed with respect to body weight, body fat, or lean body mass measured before the test session (Table 3). Similarly, food intake and fecal deposits measured during the testing session did not differ between genotypes (data not shown). Although ambulatory and vertical activity was comparable across genotype, females were more active than males during testing.

With regard to O$_2$ consumption and CO$_2$ production, interactions between gender and genotype were detected. O$_2$ consumption and CO$_2$ production for Girk4−/− males were consistently (although not significantly) larger than those measured in wild-type males, although Girk4−/− females exhibited smaller values than female wild-type animals. Mean respiratory exchange ratios (RER), however, were equivalent across groups. More importantly, a main effect of genotype on heat production was observed during periods of activity, and specifically in periods of activity during the dark phase. During these periods, wild-type mice expended significantly more energy than Girk4−/− mice. When heat production was normalized to lean body mass, main effects of genotype and gender were evident during the full session. Genotype-dependent differences were attributed primarily to differences observed in periods of activity during the dark phase, when wild-type animals expended more energy than Girk4−/− mice. Thus, despite their elevated core body temperatures and resting heart rates, Girk4−/− mice exhibited reduced overall energy expenditure.

Discussion

Recently, Tordoff and colleagues (19) compiled body-weight information on ≈2,000 viable knockout mouse strains. They discovered that although lean phenotypes are commonly observed in knockout mice (31% of all lines evaluated), only ≈3% of knockout lines weighed more than wild-type controls. Some of these mouse knockout models of obesity manifest massive overweight at an early age, such as mice lacking the melanocortin 4 receptor or leptin receptor (20, 21). Some knockout mice, including mice lacking the *tubby* candidate gene, develop obesity with age (22). These lines may be particularly helpful as we seek to understand the doubling in prevalence of human obesity between 20 and 50 years of age (23). Here, we report that Girk4−/− mice are predisposed to moderate (25%) late-onset obesity. To the best of our knowledge, this is only the second report of knockout model of obesity involving ion channel ablation. Mice lacking the *Kir6.2/Kcnj11* gene, which contributes to formation of the K$_{ATP}$ channel, have been shown in one but not another study to evince a mild (10%) overweight phenotype (24, 25).

Girk4−/− mice exhibited significantly lower net energy expenditure than wild-type control mice at 3–4 months of age, before the onset of overweight. As such, reduced energy expenditure should be considered a causative factor in the development of obesity in Girk4−/− mice. It is also noteworthy that Girk4−/− mice exhibited a mild tachycardia and elevated core body temperature between 3 and 9 months of age. Given the known distribution and role of GIRK4 in the heart, it seems reasonable to postulate that the elevated heart rate (and perhaps core body temperature) reflected a loss of I$_{KACh}$. Because cardiac output contributes to heat production, one would predict that energy expenditure would have been even lower in Girk4−/− mice had cardiac output been normal.

Girk4−/− mice also exhibited slightly elevated food intake relative to wild-type controls and out-performed wild-type counterparts in an operant test involving food. With regard to operant performance, genotype-dependent differences were prominent during progressive ratio scheduling, which is thought to probe the reinforcing efficacy of natural and drug rewards. *Girk4* expression has been studied in brain regions linked to reinforcement, including the prefrontal cortex (PFc), nucleus accumbens (NAc), and ventral
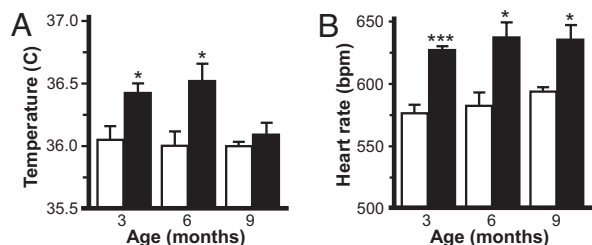
Fig. 5. Body temperature and heart rate in wild-type and Girk4−/− mice. (A) Core body temperature in male wild-type and Girk4−/− mice over a 6-h interval at 3, 6, and 9 months of age. (B) Heart rate [beat per minute (bpm)] measured over the same 6-h interval. Groups ranged from 8 to 11 per genotype and time point. * and ***, $P < 0.05$ and 0.001, respectively, vs. wild-type.

Table 3. Energy expenditure

Parameter	Male Wild-type	Male Girk4⁻/⁻	Female Wild-type	Female Girk4⁻/⁻	Main Effects Gender	Main Effects Genotype
Body mass, g	27.3 ± 1.5	29.1 ± 1.4	22.7 ± 0.7‡	23.8 ± 0.6‡	M > F***	
Body fat, g	3.1 ± 0.3	4.4 ± 0.7	3.1 ± 0.3	3.0 ± 0.3		
Lean body mass, g	20.8 ± 1.2	20.8 ± 0.8	16.9 ± 0.5‡	18.1 ± 0.5‡	M > F***	
Ambulation (×1,000)	41.5 ± 4.9	41.8 ± 3.4	57.1 ± 4.4‡	44.0 ± 3.5†	M < F*	
Vertical activity (×1,000)	3.0 ± 0.7	2.6 ± 0.4	5.2 ± 0.8‡	3.2 ± 0.4†	M < F*	
O₂ consumption, L	57.5 ± 1.0	63.0 ± 2.3	65.5 ± 1.8‡	57.1 ± 2.3†‡		interaction
Light	25.5 ± 0.9	27.8 ± 1.2	28.5 ± 1.0	24.8 ± 1.0†		interaction
Dark	32.0 ± 0.3	35.2 ± 1.3	36.9 ± 1.0‡	32.2 ± 1.5†		interaction
CO₂ production (L)	52.8 ± 1.2	57.9 ± 1.9	58.9 ± 1.6‡	52.0 ± 2.3†‡		interaction
Light	22.4 ± 1.0	24.4 ± 1.1	25.0 ± 0.8	22.2 ± 1.0†		interaction
Dark	30.4 ± 0.5	33.4 ± 1.0	33.9 ± 0.8‡	29.9 ± 1.5†‡		interaction
RER	0.91 ± 0.01	0.92 ± 0.01	0.90 ± 0.02	0.91 ± 0.02		
Heat, kcal	7.5 ± 0.3	7.1 ± 0.2	7.8 ± 0.2	7.1 ± 0.4		
Active	4.0 ± 0.3	3.8 ± 0.2	4.6 ± 0.2	3.8 ± 0.2		WT > KO*
Light	1.6 ± 0.2	1.4 ± 0.1	1.7 ± 0.1	1.5 ± 0.2		
Dark	2.4 ± 0.2	2.3 ± 0.1	2.9 ± 0.2	2.2 ± 0.1†		WT > KO*
Rest	3.5 ± 0.1	3.3 ± 0.2	3.2 ± 0.2	3.4 ± 0.3		
Normalized heat, kcal/g	0.37 ± 0.03	0.34 ± 0.01	0.46 ± 0.02‡	0.40 ± 0.02†	M < F**	WT > KO*
Active	0.20 ± 0.03	0.18 ± 0.01	0.27 ± 0.01‡	0.21 ± 0.01†	M < F**	WT > KO*
Light	0.08 ± 0.01	0.07 ± 0.01	0.10 ± 0.01	0.09 ± 0.01	M < F*	
Dark	0.12 ± 0.01	0.11 ± 0.01	0.17 ± 0.01‡	0.12 ± 0.01†	M < F**	WT > KO**
Rest	0.17 ± 0.01	0.16 ± 0.01	0.19 ± 0.01	0.19 ± 0.02		

Subjects were evaluated between 12–16 weeks of age ($n = 6–8$ per genotype and gender). Body weight and composition were determined prior to testing. Activity data are presented as infrared beam breaks. Raw and normalized (to lean body mass) heat (kcal) values are presented. Columns on the right indicate when a main effect of genotype or gender was observed. The nature of the main effect is denoted using the following abbreviations: male (M), female (F), wild-type (WT), and $Girk4^{-/-}$ (KO). *, $P < 0.05$; **, $P < 0.01$; ***, $P < 0.001$. With respect to O₂ consumption and CO₂ production, no main effect of genotype or gender was observed, though significant genotype x gender interactions were detected ($P < 0.01$ in all cases). Results of pair-wise comparisons are noted next to the appropriate value in the table: †, $P < 0.05$ vs. wild-type, same gender; ‡, $P < 0.05$ vs. male, same genotype. Differences between male and female mice of different genotypes are not reported in this table.

tegmental area (VTA). *Girk4* expression was not detected in the NAc (3, 8). In sections from Tg(*Kcnj5*-EGFP)49Gsat mice, weak and diffuse EGFP labeling was observed in neuropil of the NAc, VTA, and PFc (data not shown). In the VTA, as was seen in the substantia nigra, a small number of cell bodies were EGFP-positive (data not shown). Thus, GIRK4-containing channels may modulate the excitability of a small fraction of VTA neurons. The VTA and NAc also receive input from the VMN (26, 27). Thus, hypothalamic GIRK4-containing channels may indirectly modulate reward-relevant signaling in the mesocorticolimbic dopamine system.

It is somewhat difficult to reconcile the enhanced motivation to work for food in the operant study with the small (typically insignificant) genotype-dependent differences in daily home-cage food intake. Indeed, genotype-dependent differences were clearly evident in short test sessions (3 h) during the operant study, whereas such differences were difficult to detect in prolonged assessments of home-cage food intake. We speculate that this inconsistency relates to study-dependent differences in food availability and/or composition. Operant performance was assessed under conditions of mild food restriction and involved small palatable food pellets. Thus, genotype-dependent differences related to food size, palatability, and/or food restriction could explain the robust food-maintained operant responding and slightly elevated home-cage food intake seen in single-housed *Girk4*⁻/⁻ mice. Future studies exploring operant performance for food of distinct composition, as well as analysis of the physiological responses to food restriction, should clarify this important issue.

Given its otherwise limited tissue distribution, the conspicuous expression of *Girk4* in hypothalamic nuclei mediating energy homeostasis suggests an anatomic basis for the observed phenotype. Furthermore, GIRK channels have been implicated in the postsynaptic inhibitory effect of inhibitory transmitters on many hypothalamic neuron subtypes (11, 28, 29). Thus, it is useful to consider the impact of GIRK channel ablation on these neuron populations and energy balance. Inhibition of POMC and VMN neurons, for example, promotes food intake and reduces energy expenditure (9, 30). Loss of GIRK channels in these neurons should, therefore, inhibit food intake and enhance energy expenditure. Conversely, the inhibition of NPY neurons suppresses food intake (e.g. ref. 31). Loss of GIRK channels in this neuron population should, therefore, lead to elevated food intake and reduced energy expenditure. Our observations are more consistent with the latter scenario, but do not preclude roles for GIRK4-containing channels in neuron populations exerting opposing influences on intake and expenditure. As we pursue a detailed understanding of the adult-onset obesity in *Girk4*⁻/⁻ mice, we will need to determine the subunit composition(s) of GIRK channels in hypothalamic neurons and discern the electrophysiological consequences of subunit ablation in each neuron type. We also need to consider that the loss of *Girk4* in other brain regions or peripheral tissues, including the heart, may be responsible for some or all of the observed adult-onset weight gain.

In summary, we report a significant contribution of GIRK channels to energy homeostasis in mice. Our data specifically implicate the GIRK4 subunit in signaling pertinent to energy expenditure and food intake. Given the restricted expression pattern of the *Girk4* gene, pharmacologic and/or genetic strategies aimed at GIRK4-containing channels warrant consideration as approaches to treat or prevent obesity.

Materials and Methods

Animals. Animal use was approved by the Institutional Animal Care and Use Committee of the University of Minnesota. Unless noted, mice were group-housed (two to four same-sex siblings) on a 12-h light/dark cycle with food and water available ad libitum. The generation of *Girk4*⁻/⁻ mice is described in ref. 14. The *Girk4* null mutation was backcrossed for 22 generations to the C57BL/6J inbred strain before initiating this study. Litters of wild-type and *Girk4*⁻/⁻ mice were generated by crossing wild-type or *Girk4*⁻/⁻ parents, which were generated in crosses of *Girk4*⁺/⁻ mice. The Tg(*Kcnj5*-EGFP)49Gsat mouse was obtained from the Mutant Mouse Regional Resource Center.

Histochemistry and Microscopy. Histochemistry involving brain sections from adult mice (8–10 weeks old) was performed as described in ref. 13. Images were collected by using a Bio-Rad MRC 1024 confocal laserhead on an upright microscope and an Olympus AX-70 camera with Bio-Rad LaserSharp 3.0 software. Adobe Photoshop v.6.0 (Adobe Systems) was used to add color to images.

Longitudinal Studies. Two cohorts of mice were evaluated. Cohort 1 consisted of group-housed wild-type and *Girk4*$^{-/-}$ mice fed standard rodent chow (#2018; Harlan Teklad Global Diets) from weaning to 1 year of age. Body weights were measured biweekly from 3 weeks to 3 months of age, and then again at 6, 9, and 12 months. A representative subset of 12-month-old male wild-type and *Girk4*$^{-/-}$ mice from cohort 1 were killed for analysis of body fat content by Soxhlet extraction, a service provided by Covance Laboratories. Cohort 2 consisted of wild-type and *Girk4*$^{-/-}$ mice transferred to single-housing at 8 weeks and fed standard rodent chow throughout the study. Body weights and weekly food intake were measured between 12 and 36 weeks. For both studies, body weights were measured between 0800 and 1200 hours during routine cage refreshment.

Operant Performance. Male wild-type and *Girk4*$^{-/-}$ mice (8–12 weeks) were evaluated in a three-phase food-maintained operant test using palatable food pellets (20 mg, PJA/100020 dust-free, Noyes Precision Pellets; Research Diets) as described in ref. 18. Body weights were measured before study and were considered to be free-feeding weights.

Telemetry. Body temperature and heart rate were measured in male wild-type and *Girk4*$^{-/-}$ mice at 3, 6, and 9 months of age by using implantable radio-transmitters (Data Sciences International) as described in ref. 6. Animals were tested at one time point only. Mice were allowed to recover for 7 d after transmitter-implantation surgery. Heart rates and body temperatures were determined by averaging data obtained over 6 h of recording on day 8 (1000–1600 hours).

Indirect Calorimetry. Energy expenditure was determined in group-housed mice at 12–16 weeks of age. Experiments were performed with a single-chamber, open-circuit indirect calorimeter (Columbus Instruments) customized to permit the simultaneous measurement of O_2 consumption, CO_2 production, and activity (32). The chamber (inner dimensions: 4.25 inches $\times$ 8 inches $\times$ 5 inches; 2-liter volume) and recording equipment were housed in a dedicated room. Calibration of gas sensors was performed for each run with

a primary gas standard. Chamber airflow was maintained at 0.6 liter/min, and experiments were performed at 22°C. One day (24 h) before testing, subjects were transferred to a duplicate metabolic chamber for acclimation to the testing environment. Subsequently, mice were transferred to the metabolic chamber connected to oxygen (O_2) and carbon dioxide (CO_2) sensors for evaluation of energy expenditure. Standard rodent chow and water were available ad libitum during acclimation and testing.

Body composition was determined by using an EchoMRI body composition analyzer (Echo Medical Systems) before and after testing. Body weights were also measured just before and after testing, and changes in body weight or composition, as well as food intake and fecal output, were evaluated during the test session. Sessions began in the middle of the light cycle (1100 h) and continued through the middle of the light cycle on day 2 (1000 h). The first 30 min of data were discarded to minimize the impact of stress on expenditure indices. Every 30 min, a baseline room air measurement was taken, while VO_2 and VCO_2 were measured during 120 sequential 15-s epochs. The respiratory exchange ratio (RER) was calculated as VCO_2/VO_2. Heat produced was calculated as described in ref. 32. Ambulatory and vertical counts were tabulated throughout the session. Subjects were considered to have been at rest during a 15-s epoch if there were no ambulatory or vertical counts. Otherwise, subjects were considered to have been active. O_2 consumption, CO_2 production, and heat production were quantified for the total testing period, during periods of rest or activity, and during light and dark cycles.

Statistical Analysis. Data are expressed as the mean $\pm$ SEM. Statistical analyses were performed with the programs GraphPad Prism v.5.0 (GraphPad Software), StatView v.5.0 (SAS Institute), and SAS PROC MIXED (SAS Institute). The impact of gender and/or genotype on body weight and food intake was evaluated by using a combination of descriptive analysis and linear growth curve models. Operant performance of male wild-type and *Girk4*$^{-/-}$ mice was compared by using Student's *t* test. Body composition, energy expenditure, and related indices were compared by two-factor ANOVA, with genotype and gender as independent variables. When significant main effects or interactions were observed, data were then analyzed by using Fisher's PLSD. Significance was set at $P < 0.05$.

1. North A (1989) Drug receptors and the inhibition of nerve cells. *Br J Pharmacol* 98:13–28.
2. Logothetis DE, Kurachi Y, Galper J, Neer EJ, Clapham DE (1987) The $\beta\gamma$ subunits of GTP-binding proteins activate the muscarinic K$^+$ channel in heart. *Nature* 325:321–326.
3. Karschin C, Dissmann E, Stuhmer W, Karschin A (1996) IRK(1–3) and GIRK(1–4) inwardly rectifying K$^+$ channel mRNAs are differentially expressed in the adult rat brain. *J Neurosci* 16:3559–3570.
4. Krapivinsky G, et al. (1995) The G-protein-gated atrial K$^+$ channel I$_{KACh}$ is a heteromultimer of two inwardly rectifying K$^+$-channel proteins. *Nature* 374:135–141.
5. Koyrakh L, et al. (2005) Molecular and cellular diversity of neuronal G-protein-gated potassium channels. *J Neurosci* 25:11468–11478.
6. Bettahi I, Marker CL, Roman MI, Wickman K (2002) Contribution of the Kir3.1 subunit to the muscarinic-gated atrial potassium channel I$_{KACh}$. *J Biol Chem* 277:48282–48288.
7. Wickman K, Seldin MF, Gendler SJ, Clapham DE (1997) Partial structure, chromosome localization, and expression of the mouse Girk4 gene. *Genomics* 40:395–401.
8. Wickman K, Karschin C, Karschin A, Picciotto MR, Clapham DE (2000) Brain localization and behavioral impact of the G-protein-gated K$^+$ channel subunit GIRK4. *J Neurosci* 20:5608–5615.
9. King BM (2006) The rise, fall, and resurrection of the ventromedial hypothalamus in the regulation of feeding behavior and body weight. *Physiol Behav* 87:221–244.
10. Gao Q, Horvath TL (2008) Neuronal control of energy homeostasis. *FEBS Lett* 582:132–141.
11. Roseberry AG, Liu H, Jackson AC, Cai X, Friedman JM (2004) Neuropeptide Y-mediated inhibition of proopiomelanocortin neurons in the arcuate nucleus shows enhanced desensitization in ob/ob mice. *Neuron* 41:711–722.
12. Acuna-Goycolea C, Tamamaki N, Yanagawa Y, Obata K, van den Pol AN (2005) Mechanisms of neuropeptide Y, peptide YY, and pancreatic polypeptide inhibition of identified green fluorescent protein-expressing GABA neurons in the hypothalamic neuroendocrine arcuate nucleus. *J Neurosci* 25:7406–7419.
13. Aguado C, et al. (2008) Cell type-specific subunit composition of G-protein-gated potassium channels in the cerebellum. *J Neurochem*, in press.
14. Wickman K, Nemec J, Gendler SJ, Clapham DE (1998) Abnormal heart rate regulation in GIRK4 knockout mice. *Neuron* 20:103–114.
15. Reed DR, Bachmanov AA, Tordoff MG (2007) Forty mouse strain survey of body composition. *Physiol Behav* 91:593–600.
16. Voikar V, Polus A, Vasar E, Rauvala H (2005) Long-term individual housing in C57BL/6J and DBA/2 mice: Assessment of behavioral consequences. *Genes Brain Behav* 4:240–252.
17. Yamada K, Ohki-Hamazaki H, Wada K (2000) Differential effects of social isolation upon body weight, food consumption, and responsiveness to novel and social environment in bombesin receptor subtype-3 (BRS-3) deficient mice. *Physiol Behav* 68:555–561.
18. Pravetoni M, Wickman K (2008) Behavioral characterization of mice lacking GIRK/Kir3 channel subunits. *Genes Brain Behav*, in press.
19. Reed DR, Lawler MP, Tordoff MG (2008) Reduced body weight is a common effect of gene knockout in mice. *BMC Genet* 9:4.
20. Abdelilah-Seyfried S, et al. (2000) A gain-of-function screen for genes that affect the development of the Drosophila adult external sensory organ. *Genetics* 155:733–752.
21. Cohen P, et al. (2001) Selective deletion of leptin receptor in neurons leads to obesity. *J Clin Invest* 108:1113–1121.
22. Stubdal H, et al. (2000) Targeted deletion of the tub mouse obesity gene reveals that tubby is a loss-of-function mutation. *Mol Cell Biol* 20:878–882.
23. Seidell JC, Flegal KM (1997) Assessing obesity: Classification and epidemiology. *Br Med Bull* 53:238–252.
24. Miki T, et al. (1998) Defective insulin secretion and enhanced insulin action in K$_{ATP}$ channel-deficient mice. *Proc Natl Acad Sci USA* 95:10402–10406.
25. Kanezaki Y, et al. (2004) K$_{ATP}$ channel knockout mice crossbred with transgenic mice expressing a dominant-negative form of human insulin receptor have glucose intolerance but not diabetes. *Endocr J* 51:133–144.
26. Saper CB, Swanson LW, Cowan WM (1976) The efferent connections of the ventromedial nucleus of the hypothalamus of the rat. *J Comp Neurol* 169:409–442.
27. Canteras NS, Simerly RB, Swanson LW (1994) Organization of projections from the ventromedial nucleus of the hypothalamus: A Phaseolus vulgaris-leucoagglutinin study in the rat. *J Comp Neurol* 348:41–79.
28. Priestley T (1992) The effect of baclofen and somatostatin on neuronal activity in the rat ventromedial hypothalamic nucleus in vitro. *Neuropharmacology* 31:103–109.
29. Acuna-Goycolea C, van den Pol AN (2005) Peptide YY(3–36) inhibits both anorexigenic proopiomelanocortin and orexigenic neuropeptide Y neurons: Implications for hypothalamic regulation of energy homeostasis. *J Neurosci* 25:10510–10519.
30. Balthasar N (2006) Genetic dissection of neuronal pathways controlling energy homeostasis. *Obesity (Silver Spring)* 14(Suppl 5):222S–227S.
31. Heisler LK, et al. (2006) Serotonin reciprocally regulates melanocortin neurons to modulate food intake. *Neuron* 51:239–249.
32. Wang C, Bomberg E, Billington C, Levine A, Kotz CM (2007) Brain-derived neurotrophic factor in the hypothalamic paraventricular nucleus increases energy expenditure by elevating metabolic rate. *Am J Physiol* 293:R992–R1002.
33. Halasy K, Somogyi P (1993) Subdivisions in the multiple GABAergic innervation of granule cells in the dentate gyrus of the rat hippocampus. *Eur J Neurosci* 5:411–429.
34. Franklin K, Paxinos G (1997) *The Mouse Brain in Stereotaxic Coordinates* (Academic, New York).

PHYSIOLOGY

Perry *et al.*